http://dx.doi.org/10.5935/0103-5053.20150306

J. Braz. Chem. Soc., Vol. 27, No. 2, 402-410, 2016.
Printed in Brazil - ©2016 Sociedade Brasileira de Química
0103 - 5053 $6.00+0.00

Article

Synthesis, Physicochemical and Photophysical Characterization of 4-(1-Pyrenyl)-butyl-α-*D*-mannopyranoside

Catalina Sandoval,[a] Franco S. Arriagada,[a] Julio R. De la Fuente,[a] Susana A. Sanchez,[b] Javier Morales,[c] Nancy Pizarro,[d] Santi Nonell[e] and German Gunther*[,a]

[a]*Departamento de Química Orgánica y Físico Química, Facultad de Ciencias Químicas y Farmacéuticas, Universidad de Chile*

[b]*Departamento de Polímeros, Facultad de Ciencias Químicas, Universidad de Concepción, Edmundo Larenas 129, Chile*

[c]*Departamento de Ciencias y Tecnología Farmacéutica, Facultad de Ciencias Químicas y Farmacéuticas, Universidad de Chile*

[d]*Departamento de Ciencias Quimicas, Facultad de Ciencias Exactas, Universidad Andres Bello, Av. República 275, 3er Piso, Santiago, Chile*

[e]*Institut Quimic de Sarria, Universitat Ramon Llull, Via Augusta, 390, 08017 Barcelona, Spain*

Glycolipids are biomolecules composed of a lipid chain (lipophilic) and a monosaccharide or oligosaccharide as hydrophilic group. Their chemical structure and biological role make them undoubtedly good candidates for a large and continuously growing number of biotechnological applications. Mannose is a carbohydrate present on membrane glycolipids of a wide number of pathogenic microorganisms (bacteria, fungi, protozoa, and viruses) and specifically recognized by several lectins. We synthesized a mannose derivative linked through a short methylene chain to a pyrene moiety which behaves as a surfactant, able to aggregate, and retains the photophysical properties of pyrene: showing comparable absorption and emission spectra, having lower fluorescence quantum yield and the ability to form excimer, and finally the ability to produce $O_2(^1\Delta_g)$ with high quantum yields. Thus, this novel molecule would open future applications for detection (fluorescence) or inactivation (singlet oxygen) of bacterial pathogens, viruses, tumor cells, or particular cells.

Keywords: pyrene, mannose, excimer, singlet oxygen, micelles

Introduction

A great number of biological processes involving cell-cell interactions (signaling, recognition and adhesion) are modulated by sugar molecules located on the cell surface as glycoconjugates. Several physiologically important functions involve the participation of glycans or glycolipids, among them normal embryonic development, host-pathogen interaction during infection, host immune response, disease development, metastasis, intracellular trafficking and localization, rate of degradation and membrane rigidity.[1-9]

Glycolipids are biomolecules composed of a lipid chain (lipophilic) and a monosaccharide or oligosaccharide as hydrophilic group. They are generally non-toxic, easily degradable and their solubility is good in water and organic solvents.[10] The most common glycolipids contain galactose, mannose, fucose, glucose, glucosamine, galactosamine, or sialic acid.[11] Considering the chemical structure and the biological role of the glycolipids, they undoubtedly are good candidates for a large and continuously growing number of biotechnological applications, such as thermotropic and lyotropic liquid crystals,[12,13] surfactants,[14] lubricants,[10] cosmetics,[15,16] and membrane solubilizing agents[17-19] among others.

Mannose is a carbohydrate present on membrane glycolipids of a wide number of pathogenic microorganisms (bacteria, fungi, protozoa, and viruses). As a consequence, there is a defensive mechanism, for trapping and destroying the invasive microorganism, based on the specific recognition of this particular monosaccharide, involving the protein mannose-binding lectin (MLB).[20] There are also

*e-mail: ggunther@ciq.uchile.cl

reports that pathogens like *E. coli* (involved in most urinary infections) are able to recognize the mannose located on the surface of urinary bladder to initiate the infection process.[21] Mannopyranoside alkyl derivatives are known to have antibacterial activity[22] and successful attempts to photoinactivate *P. aeruginosa* have been achieved with mannose functionalized nanoparticles.[23]

The amphiphilic nature of glycolipids allows them to spontaneously aggregate and form structures like micelles,[24] and there are also reports on their capacity to form bilayers and/or vesicles.[25] Many reports on the aggregation capabilities of glycolipids alkyl polyglycosides, sorbitan esters, and sucrose esters can be found in literature.[26-30]

We are interested in adding fluorescent properties and photosensitizing properties to glycolipids by chemically attaching a fluorescent moiety on its structure. Our choice is pyrene, a commonly used fluorescent probe and efficient singlet oxygen, $O_2(^1\Delta_g)$, photosensitizer. Pyrene and other dyes have been employed to modify molecules with a wide range of possible applications: (*i*) as photolabile protection groups. Esterification of carboxylic acids yielded the fluorescent 1-pyrenylmethyl esters, which when photolyzed at 340 nm are able to re-generate the starting acids in high yield;[31] (*ii*) as an amphiphilic fluorescent probe. Aggregation properties of pyrenyl derivatives of pyrrolidynium surfactants with different hydrophilic lipophilic balance (HLB) have been studied;[32] (*iii*) as a label for lipids. In pyrene phospolipids, the bulky chromophore is usually attached to the end of one of the acyl chains, where the properties of the labeled lipid are significantly modified despite its hydrophobicity;[33-35] (*iv*) as functionalized low molecular weight gelators that fluoresce and have the ability to effectively bind with single walled carbon nanotubes (SWCNTs).[36]

In the present study we synthesized a mannose derivative linked through a short methylene chain to a pyrene moiety with the purpose of adding fluorescent properties to the mannose compound. Although this novel pyrene-mannose conjugate showed lower fluorescence quantum yields than other pyrene molecules bearing substituents at position 2, its ability to form excimers as well as to generate $O_2(^1\Delta_g)$ remains unaltered. Thus, the behavior of this novel molecule would open future applications for detection (fluorescence) or inactivation ($O_2(^1\Delta_g)$) of bacterial pathogens, viruses, tumor cells, or other particular cells.

Experimental

All solvents employed were of high performance liquid chromatography (HPLC) quality, reagents employed were analytical grade and they were employed with no further purification unless otherwise stated. 1-Palmitoyl-2-oleoyl-*sn*-glycero-3-phosphocholine (POPC) from Sigma was used as received. Dioctadecyldimethylammonium chloride (DODAC) from Herga Ind. was purified as described elsewhere.[37]

Synthesis of 4-(1-pyrenyl)-butyl-α-*D*-mannopyranoside

1-Pyrenebutanol (50 mmol) was added to a solution containing 10 mmol of mannose peracetate (1,2,3,4,6-penta-*O*-acetyl-α-*D*-mannopyranose) in 70 mL of dry dichloromethane. After stirring the mixture during 20 min on an ice bath, the complex BF_3OEt_2 (100 mmol) was added dropwise. The mixture was stirred at room temperature during 24 h. After this time 50 mL of dichloromethane were added and the mixture was poured into ice cold water. The organic phase was separated and washed with saturated $NaHCO_3$, followed by water and finally dried with Na_2SO_4 prior to filtration and concentration. The reaction product was purified using silica column chromatography, with benzene/ethyl acetate starting with a 5:1 mixture and ending with a 2.5:1 mixture. The substituted peracetylated saccharide (0.2 g) was dissolved in MeOH/CH_2Cl_2 (4:1, 10 mL), and 0.5 mL of freshly prepared MeONa (1 mol L^{-1}) were added. The mixture was stirred at room temperature for 24 h. The reaction product was neutralized with Amberlyst 15, and finally concentrated. Purification was made by column chromatography with dichloromethane/methanol as mobile phase at two successive different proportions (10:1 and 5:1) to obtain pure 4-(1-pyrenyl)-butyl-α-*D*-mannopyranoside (Manpy, see Figure 1). ^{1}H nuclear magnetic resonance (NMR) data of acetyl protected and pure Manpy are shown in Supplementary Information.

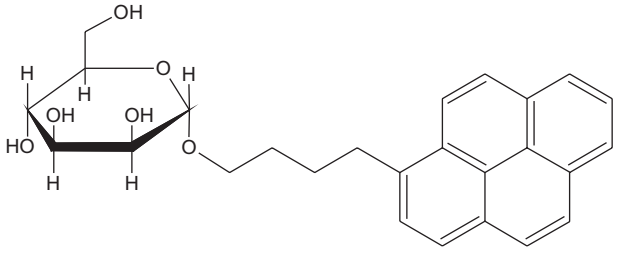

Figure 1. Chemical structure of 4-(1-pyrenyl)-butyl-α-*D*-mannopyranoside (Manpy).

Spectroscopic and photophysical measurements

UV-Vis spectra were recorded on an Agilent 8453 diode-array spectrophotometer in the range of 250-700 nm. Emission spectra were measured in an ISS PC1 spectrofluorometer at room temperature. Luminescence

lifetime measurements were carried out with the time correlated single photon counting (TCSPC) technique using a PicoQuant Fluotime 200 fluorescence lifetime spectrometer with a multichannel scaler (PicoQuant Timeharp 250), employing as excitation source at 331 nm a PLS-8-2-465 light-emitting diode (LED). Fluorescence quantum yields were measured in a FluoroMax 4CP (Horiba Jovin Yvon) spectrofluorimeter equipped with the Quanta-Phi integrating sphere.

$O_2(^1\Delta_g)$ lifetime decays were acquired with a Fluotime 200 consisting of a Nanoharp 200 multichannel scaler. Excitation at 355 nm was achieved with a FTSS355-Q3 laser (Crystal Laser) working at 1 kHz repetition rate. For the detection at 1270 nm a NIR PMT H10330A (Hamamatsu) was employed. The $O_2(^1\Delta_g)$ quantum yields (Φ_Δ) were determined by comparing the intensity of the 1270 nm signals to those of optically-matched solutions of phenalelone as reference.[38]

Nanosecond laser flash photolysis experiments were performed on argon saturated dichloromethane solutions by exciting at 355 nm and sweeping the absorption spectra between 400 and 600 nm. The instrument was described previously;[39] some additional accessories are now available: excitation with a Continuum Surelite I 10 Hz Q-switched Nd-YAG laser and signal collection with a WaveSurfer 600 MHz LeCroy oscilloscope. Software written in National Instruments LabView 8.0[40] controls the laser, monochromator and shutters; captured data are fed to an Igor Pro 6.3[41] written program for treatment and display.

Critical micellar concentration measurements

The values for the critical micellar concentration (cmc) were determined by employing three methods: UV-Vis absorbance, fluorescence (using the same mannose derivative as probe) and surface tension measurements. Surface tension measurements were performed with a DuNoüy tensiometer (K8 Krüss, measurement range 5-90 mN m^{-1} with Pt/Ir ring of 20 mm). From plots of the change in absorbance, emission intensity or surface tension values against surfactant concentration, cmc was determined from the point of slope change. All described measurements were performed at 25.0 ± 0.1 ºC.

Small unilamellar vesicles/liposomes (SUVs) preparation

Small unilamellar liposomes (SUVs) of DODAC or POPC were obtained by ultrasonication of lipids suspensions (1 to 5 mmol L^{-1}) in pH 7.4 buffer phosphate, with a Cole Parmer ultrasonic homogenizer.

Results and Discussion

Steady state absorption and emission spectra

Absorption and emission spectra of Manpy in chloroform and water show the common shape for pyrene derivatives monosubstituted at position 2 (Figure 2).[42] Absorption spectra display the typical low intensity and vibrationally-resolved band between 360 and 400 nm corresponding to $S_0 \rightarrow S_1$ transition (as can be seen in Figure 2, inset), a second more intense group of bands between 300 and 350 nm corresponding to $S_0 \rightarrow S_2$ transition, and a third set of bands at shorter wavelengths belong to the $S_0 \rightarrow S_3$ transition.[42] The emission spectra show likewise the well known features of the pyrene monomer spectrum, namely two main peaks at 380 and 400 nm (Figure 2).[42] Both absorption and fluorescence spectra show a small red shift in chloroform relative to water.

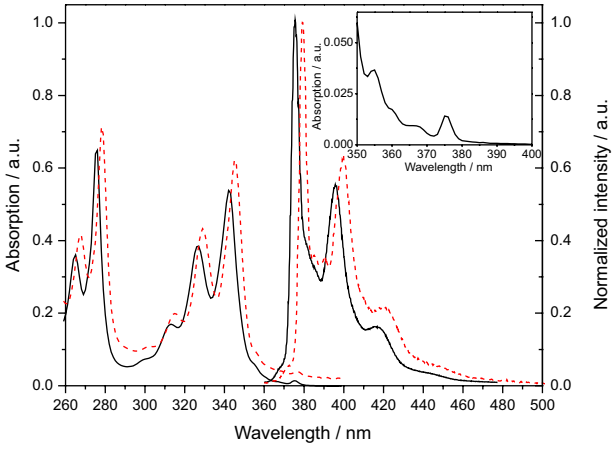

Figure 2. Absorption and normalized emission spectra of Manpy in water (—) and chloroform (– –). Inset corresponds to Manpy absorption in water, between 350 and 400 nm.

Fluorescence quantum yields of Manpy were determined in several non-aqueous solvents as a function of concentration (Table 1). For non-aqueous solvents the values were smaller (under 0.100) than those reported for several 2-alkyl pyrenes (in the range from 0.200 to 0.450)[42] and did not show any significant concentration dependence (in the monitored range). When the solvent was water, the fluorescence quantum yield decreased from 0.300 to 0.100 upon increasing the concentration. At the same time, formation of the pyrene excimer was clearly detected, as can be seen in Figure 3a.

Aggregation studies

The cmc value (Table 2) was determined by three different methods: by pyrene UV-Vis absorbance, by

Table 1. Molar extinction coefficients and fluorescence quantum yields of Manpy

Solvent	log ε; λ_{max} / nm	Φ_{Fl}
Methanol	4.46; 342	–
Chloroform	4.39; 344	–
Ethanol	4.50; 341	0.058
Hexane	4.36; 343	0.020
Water	4.28;[a] 342	0.10 (0.500)
		0.15 (0.175)
		0.22 (0.087)
		0.28 (0.044)
		0.31 (0.015)
		0.28 (0.005)
Benzene	4.84; 345	0.082

[a]Lower concentration employed. log ε: Molar extinction coefficients; λ_{max}: wavelength of maximum absorbance; Φ_{Fl}: fluorescence quantum yield; the values in parentheses are the mmol L^{-1} concentrations.

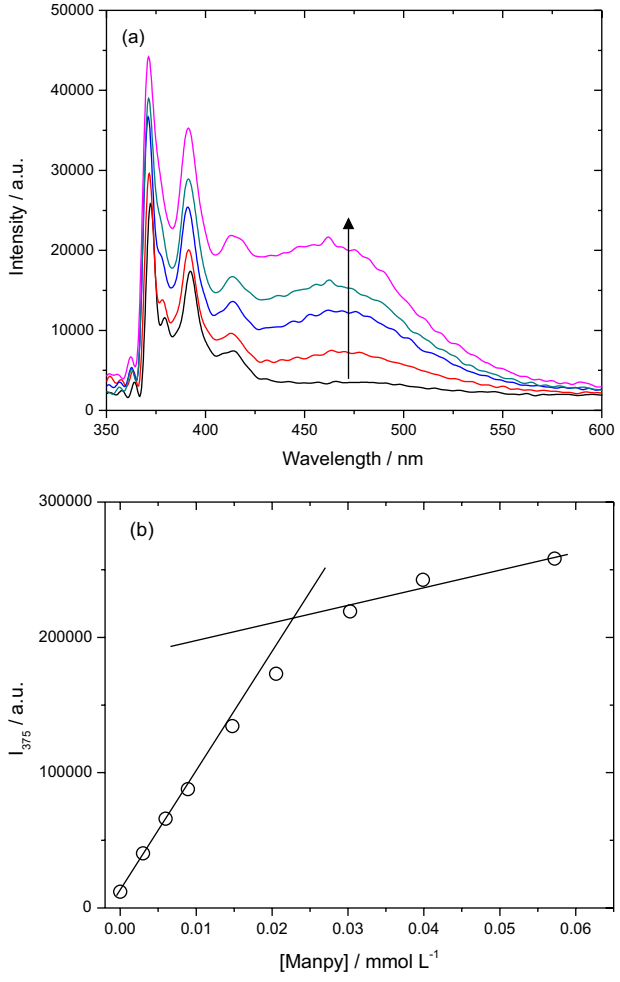

Figure 3. (a) Effect of concentration increase on the emission spectra of Manpy in water; (b) determination of Manpy cmc monitoring the change in emission intensity at 375 nm.

surface tension measurements and by pyrene fluorescent emission (including emission quantum yield, intensity and excimer formation). Figure 3b shows the cmc determination by Manpy emission at 375 nm. The cmc values determined at 25 ºC by other methodologies yielded comparable results, with the clear exception of excimer formation. In this case, the cmc was obtained from the ratio of excimer and monomer emission intensities (I_E / I_M), which seems to be inadequate likely because the probe concentration (pyrene) is increasing concomitantly with surfactant (mannose) concentration. The cmc value determined for Manpy is smaller, but on the order of the value reported for *n*-dodecyl-α-*D*-mannopyranoside (0.05 mmol L^{-1}), and much lower than the ones measured for decyl (0.25 mmol L^{-1}) and octyl (6 mmol L^{-1}) derivatives (these reported values were determined employing surface tension measurements).[22] Considering a linear dependence between HLB and cmc, as reported for families of surfactants,[43] the HLB value for Manpy would correspond to an alkyl-mannoside with between 12 and 14 methylene units.

Time resolved spectroscopy

The studied pyrene derivative has relatively long lived singlet excited states (Table 3). Singlet lifetimes values in air-saturated solvents range from 10 to 100 ns, the largest value being observed in water. In deaerated solutions the singlet state lifetimes increase by almost one order of magnitude, except in water. Figure 4 shows the monomer emission at low concentration in benzene under air (22.1 ns) and nitrogen (170.6 ns). The monoexponential decays denote the absence of excimer formation. Singlet state lifetimes in vesicles and liposomes are noticeable longer than in homogeneous media, especially for membranes below their transition temperature (20 °C) where mobility is restricted.

Singlet oxygen generation

In order to study if Manpy retains the capacity of isolated pyrene to generate $O_2(^1\Delta_g)$, photosensitization experiments were performed under several experimental conditions.

The $O_2(^1\Delta_g)$ excitation process in photosensitization involves at least two steps: photosensitizer excitation (to its singlet or triplet excited states), followed by energy transfer to molecular oxygen. For most photosensitizers, only the triplet state is capable of producing $O_2(^1\Delta_g)$ owing to its longer lifetime. However, if the lifetime of the first singlet excited state of the dye is long enough (more than 20 ns, as in our case for Manpy) and the energy gap between

Table 2. Critical micellar concentration values for Manpy measured by different methods

Methodology	UV-Vis	Surface tension	Φ_{FI}	Fluorescence intensity	I_E / I_M
cmc / (10^{-2} mmol L^{-1})	1.92 ± 0.06	1.71 ± 0.04	1.96 ± 0.02	2.23 ± 0.09	10.50 ± 0.80

cmc: Critical micellar concentration; Φ_{FI}: fluorescence quantum yield; I_E / I_M: ratio of excimer and monomer emission intensities.

Table 3. Lifetimes of singlet and triplet states of Manpy in several solvents

Solvent	Singlet state		Triplet state	
	τ_{air} / ns	τ_{N2} / ns	τ_{air} / μs	τ_{Ar} / μs
Chloroform	17.9	57.7	0.512	–
Water	101.9	125.7	–	125.6
Benzene	22.1	170.6	0.273	17.9
Ethanol	22.1	156.9	–	–
Methanol	19.0	200.6	0.280	9.2
Hexane	9.4	161.50	n.e.	–
DODAC (20 ºC)	158.0	278.9	–	–
DODAC (50 ºC)	100.3	216.1	–	–
POPC (20 ºC)	162.0	267.2	–	–
POPC (50 ºC)	99.70	211.3	–	–

τ: Lifetimes of singlet or triplet states under air (τ_{air}), nitrogen (τ_{N2}) and argon (τ_{Ar}); n.e.: not evaluated, resolution was not enough to fit signal growth; DODAC: dioctadecyldimethylammonium chloride; POPC: 1-palmitoyl-2-oleoyl-*sn*-glycero-3-phosphocholine.

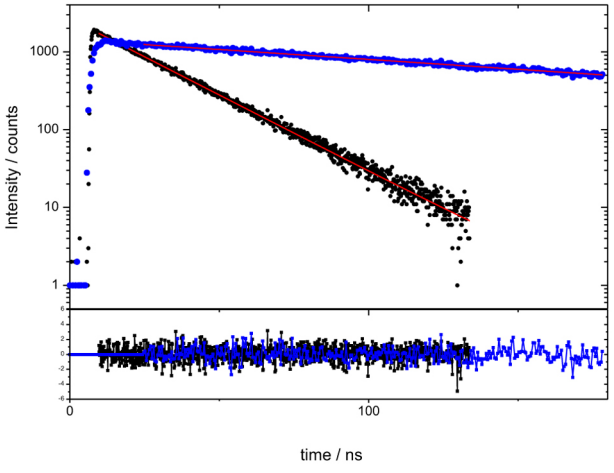

Figure 4. Emission of Manpy singlet state from purged (blue) air equilibrated benzene solution (black) with excitation wavelength equal to 331nm.

the singlet and triplet state of sensitizer is more than 22.5 kcal mol^{-1}, quenching of the singlet state by ground state molecular oxygen will also produce $O_2(^1\Delta_g)$ and the triplet state of sensitizer will be produced as result:

$$^1\text{Manpy} + O_2 \rightarrow {}^3\text{Manpy} + O_2(^1\Delta_g) \quad (1)$$

$$^3\text{Manpy} + O_2 \rightarrow \text{Manpy} + O_2(^1\Delta_g) \quad (2)$$

Under such conditions, quantum yields of $O_2(^1\Delta_g)$ generation up to 2 can be expected. Likewise, the concentration of $O_2(^1\Delta_g)$ is expected to rise and decay reflecting the singlet and triplet pathways:[44]

$$[O_2(^1{}_g)](t \quad [^1\text{Manpy}]_o \times {}^S\left({}^{-t/} \quad {}^{-t/}{}_S + \right.$$
$$[^1\text{Manpy}]_o \times {}^T\left({}^{-t/} \quad {}^{-t/}{}_T \right. \quad (3)$$

where $\Phi_\Delta{}^S$ and $\Phi_\Delta{}^T$ are the quantum yields of $O_2(^1\Delta_g)$ generation for the singlet and triplet pathways, respectively, and τ_S, τ_T and τ_Δ refer to the lifetimes of the singlet and triplet states of the photosensitizer and of $O_2(^1\Delta_g)$, respectively.

When this is the case, the infrared emission of excited oxygen obeys the following equation:

$$I(t) = A_S e^{-t/}{}_S \quad A_T e^{-t/}{}_T + (A_S + A_T) e^{-t/} \quad (4)$$

The empirical constants A_S and A_T contain instrumental factors, kinetic parameters and ground state oxygen and excited sensitizer concentrations and are proportional to the quantum yields of $O_2(^1\Delta_g)$ generation from the singlet and triplet state, respectively.[45,46]

Figure 5 shows the time dependence of $O_2(^1\Delta_g)$ phosphorescence in methanol equilibrated with air. As can be seen the signal fits properly to a tri-exponential function,

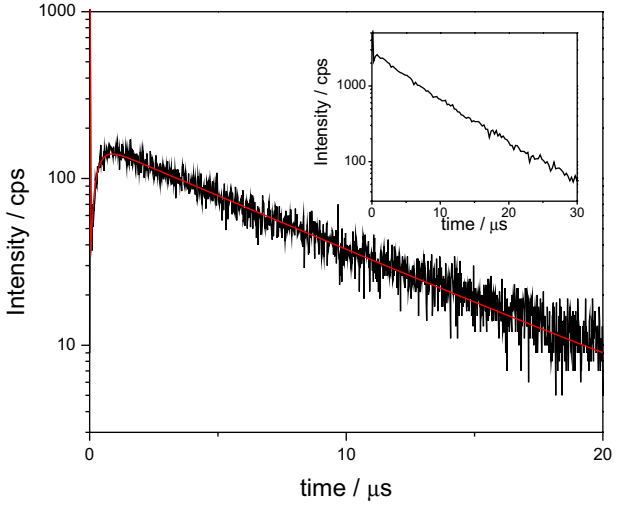

Figure 5. Infrared emission of $O_2(^1\Delta_g)$ (1270 nm) produced upon excitation of Manpy at 355 nm in air-saturated methanol. Inset corresponds to full scale decay.

which includes a very short component of scattered light convoluted with the production of $O_2(^1\Delta_g)$ from the singlet state of Manpy, an exponential growth of near 300 ns (which is assigned to the triplet state of Manpy) and a decay of 6.60 μs (assigned to $O_2(^1\Delta_g)$ lifetime); this value is shorter than the reported for it in this solvent (around 9 μs)[47] indicating that Manpy is able to quench $O_2(^1\Delta_g)$. Triplet lifetimes of Manpy in solvents equilibrated with air and indirectly measured are reported in Table 3.

The $O_2(^1\Delta_g)$ quantum yields (Φ_Δ) were determined in several solvents by comparing the total $O_2(^1\Delta_g)$ intensity ($A_S + A_T$) with that of a standard photosensitizer with known Φ_Δ. The results in Table 4 indicate a high capacity of Manpy to generate $O_2(^1\Delta_g)$ with the exception of hexane as solvent, no evidence of excimer formation was detected monitoring emission at 480 nm. Therefore, from the quantum yield for $O_2(^1\Delta_g)$ equal to 1.51, it can be concluded that both the singlet and triplet excited states of Manpy are involved in its generation. Additionally and consistently with oscillator strength of absorption bands ($S_0 \rightarrow S_1$ and $S_0 \rightarrow S_2$, as can be seen in Figure 2) it can be stated that population of the first excited singlet is more efficient through S_2 than by direct absorption.

Table 4. $O_2(^1\Delta_g)$ quantum yields values for Manpy in several solvents, determined using phenalelone as actinometer, with excitation at 355 nm under air

Solvent	Φ_Δ
Chloroform	1.51
Benzene	0.87
Methanol	1.59
Hexane	0.12

Φ_Δ: $O_2(^1\Delta_g)$ quantum yields.

Excimer formation in homogeneous and heterogeneous media

At higher probe concentrations, fluorescence decays corresponding to the monomer and excimer of Manpy can be measured. Experimental data, obtained in several solvents, were analyzed globally employing the kinetic scheme proposed by Birks *et al.*,[48] including in the analysis at least 20 decays at different wavelengths. After laser pulse excitation of sample solutions, monomer end excimer fluorescence emissions follow a bi-exponential decay, according to equations 5 and 6. As can be seen in Figure 6, monomer fluorescence decays in a few nanoseconds, and concurrently the intensity of the excimer emission increases, and then decays. Adopting Birks notation equations describing the kinetic scheme for this coupled system:

$$I_m = Ae^{-\lambda_1 t} + Be^{-\lambda_2 t} \quad (5)$$

$$I_e = D(e^{-\lambda_1 t} - e^{-\lambda_2 t}) \quad (6)$$

with:

$$_{1,2} \quad \frac{1}{2}\left(\sqrt{\quad} \right)^{2} \quad _{dm} \quad _{md} \quad (7)$$

$$X = k_{fm} + k_{dm}[Manpy] \quad (8)$$

$$Y = k_D + k_{md} \quad (9)$$

where k_{fm} and k_{fe} are the fluorescence rate constants of monomer and excimer, respectively, k_{dm} is excimer formation rate constant and k_{md} corresponds to excimer dissociation rate constant.

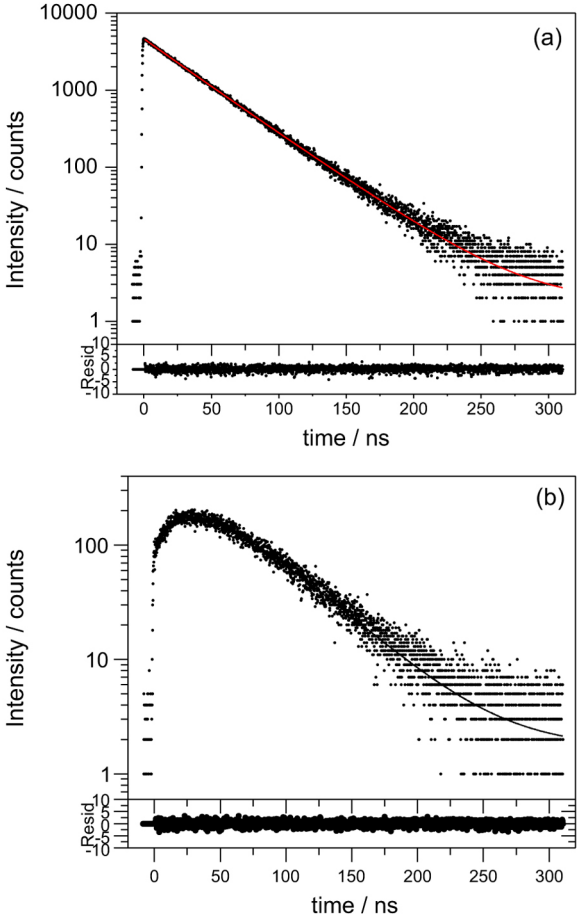

Figure 6. Emission decays followed at (a) 385 nm and at (b) 490 nm, corresponding to monomer and excimer in a coupled system.

Data fit accurately to the model equations 5 and 6, as can be seen in Figure 6. The recovered kinetic data for excimer lifetime and rate constant of excimer formation and dissociation are given in Table 5.

Lifetimes determined for Manpy excimer are of

Table 5. Photophysical parameters of Manpy excimer in several solvents

Solvent	Excimer			
	τ_{air} / ns	τ_{N2} / ns	k_{dm} (× 10^9)	k_{md} (× 10^7)
Chloroform	35.0	38.5	6.0	6.0
Benzene	63.0	64.0	6.3	6.9
Methanol	17.0	18.0	0.8	1.0
DODAC (20 ºC)	63.0	69.0	0.49	1.0
DODAC (50 ºC)	51.8	51.9	1.4	1.1
POPC (20 ºC)	154.1	160.2	0.27	1.9
POPC (50 ºC)	96.3	98.4	3.3	2.1

τ: Lifetimes under air (τ_{air}) and nitrogen (τ_{N2}); k_{dm}: excimer formation rate; k_{md}: excimer dissociation rate constant; DODAC: dioctadecyldimethylammonium chloride; POPC: 1-palmitoyl-2-oleoyl-*sn*-glycero-3-phosphocholine.

the same magnitude of pyrene excimers, being also independent of oxygen presence. The excimer formation and dissociation rate constants in homogeneous media are of the same order of magnitude as data formerly reported by Birks *et al.*[48] for non-substituted pyrene. In the case of constrained media, Manpy excimer formation rate constant k_{dm} clearly senses the difference between liquid and gel phase of membrane. In the liquid phase the two dimensional restricted diffusion yields k_{dm} constants slightly lower than in homogeneous media, while for measurements below phase transition temperature, k_{dm} values are notoriously reduced (for dipalmitoylphosphatidylcholine (DPPC) transition is reported to start at 42 ºC,[49] and 40 ºC for DODAC).[50]

Absorption laser flash photolysis

In order to fulfill the photophysical characterization of long lived species of Manpy we performed a series of absorption flash photolysis determinations.

To measure the triplet lifetime and to obtain the transient spectra, several experiments were carried out. These experiments were done in argon saturated solution at low concentration (below the cmc) in methanol, benzene and water. In argon saturated methanol (Figure 7), three spectral maxima appear, the first and third at 410 and 515 nm with a lifetime of 9.23 μs and in between, at 455 nm, with a lifetime of 19.08 μs. The absorption at 410 nm that grows with a lifetime of 220 ns should be attributed to the dye excited singlet. This growth can be associated with the singlet decay in methanol of 200.6 ns (see Table 3). The absorption band at 515 nm decays with the same lifetime, and is therefore attributed to Manpy triplet. On the other hand, the band at 455 nm might be tentatively attributed to a radical cation located in the pyrene moiety as reported in literature for other substituted pyrenes.[51-53] Interestingly, at very short times (0.2 μs) after the laser pulse, a strong emission can be observed. This emission is identical to the fluorescent emission spectrum of Manpy and is attributed to it.

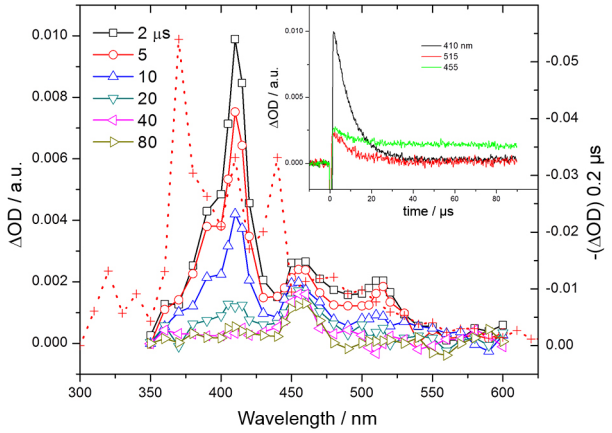

Figure 7. Transient spectra for argon saturated methanol solution of Manpy. The red + dotted spectrum shows the Manpy emission still observable 0.2 μs after the laser pulse scaled at the right axis. Inset: kinetic traces at the absorption maxima.

In argon saturated benzene the situation is similar to the one described for argon saturated methanol, with three maxima located at 420, 485 and 520 nm, respectively (see Supplementary Information). In this case also, the absorption at 420 and 485 nm decays synchronously and can be attributed to the triplet-triplet dye absorption. The absorption at 420 nm grows with a lifetime of 170 ns similar to the decay of the Manpy singlet in N_2 saturated benzene.

In water Manpy shows a different behavior with strong emission depletion between 360 and 430 nm, at times as long as 1 μs after the laser pulse (Figure 8). At longer elapsed times absorption bands appear at wavelengths of 410 and 460 nm, which can be attributed to the triplet-triplet absorption and to the pyrene radical cation, respectively. It is surprising the long lifetime, in the order of milliseconds, for the absorption at 410 nm suggesting that this absorption cannot be attributed to a common triplet. This long-lasting absorption together with the lack of structure in the emission observed before 1 μs, suggests some kind of association of Manpy molecules in water, even at concentrations below the cmc. This assumption is also supported by the differences of this emission with the Manpy fluorescence in water (Figure 2).

Conclusions

Our results show that the synthesized glycolipid Manpy retains the photophysical properties of the isolated probe, pyrene (emission and or singlet oxygen generation),

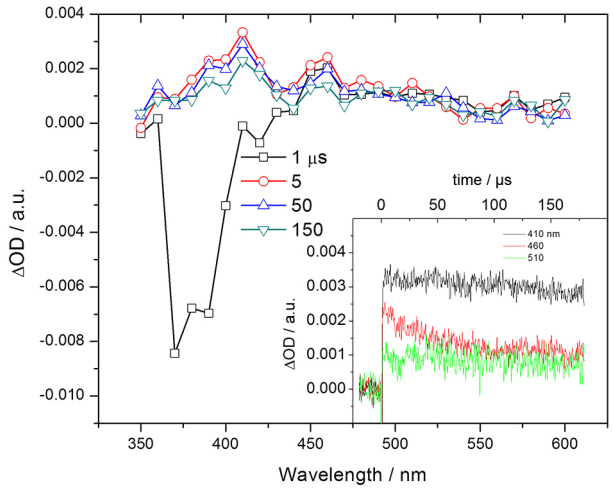

Figure 8. Transient spectra of argon saturated aqueous Manpy solution. Inset: kinetic profiles at relevant wavelengths.

independent of the mannose present as hydrophilic head. If the capacity of mannose to interact with specific lectins remains unaltered, this family of compounds could be relevant for future applications in detection (fluorescence) or inactivation (singlet oxygen) of pathogens, viruses, tumor cells, or particular cells.

Supplementary Information

Supplementary information (^{1}H NMR tables for peracetylated Manpy and Manpy; transient absorption of Manpy dissolved in argon saturated benzene) is available free of charge at http://jbcs.sbq.org.br as PDF file.

Acknowledgements

To celebrate the countless contributions of Frank H. Quina to the chemical and photochemical knowledge. This work was supported by funds from Fondecyt 1120196. C. S. thanks D. I. (University of Chile), and S. A. S. acknowledges Fondecyt 1140454.

References

1. Chammas, R.; Veiga, S. S.; Line, S.; Potocnjak, P.; Brentani, R. R.; *J. Biol. Chem.* **1991**, *266*, 3349.
2. Opdenakker, G.; Rudd, P. M.; Ponting, C. P.; Dwek, R. A.; *FASEB J.* **1993**, *7*, 1330.
3. Zheng, M. Z.; Fang, H.; Tsuruoka, T.; Tsuji, T.; Sasaki, T.; Hakomori, S.; *J. Biol. Chem.* **1993**, *268*, 2217.
4. Mody, R.; Joshi, S.; Chaney, W.; *J. Pharmacol. Toxicol.* **1995**, *33*, 1.
5. Disney, M. D.; Seeberger, P. H.; *Chem. Biol.* **2004**, *11*, 1701.
6. Nimrichter, L.; Gargir, A.; Gortler, M.; Altstock, R. T.; Shtevi, A.; Weisshaus, O.; Fire, E.; Dotan, N.; Schnaar, R. L.; *Glycobiology* **2004**, *14*, 197.
7. Blomme, B.; Van Steenkiste, C.; Callewaert, N.; Van Vlierberghe, H.; *J. Hepatol.* **2009**, *50*, 592.
8. Mukhopadhyay, B.; Martins, M. B.; Karamanska, R.; Russell, D. A.; Field, R. A.; *Tetrahedron Lett.* **2009**, *50*, 886.
9. Zachara, N. E.; Hart, G. W.; *Biochim. Biophys. Acta, Mol. Cell Biol. Lipids* **2006**, *1761*, 599.
10. Vill, V.; Hashim, R.; *Curr. Opin. Colloid Interface Sci.* **2002**, *7*, 395.
11. Dwek, R. A.; *Chem. Rev.* **1996**, *96*, 683.
12. Faivre, V.; Rosilio, V.; *Expert Opin. Drug Delivery* **2010**, *7*, 1031.
13. Gerber, S.; Wulf, M.; Milkereit, G.; Vill, V.; Howe, J.; Roessle, M.; Garidel, P.; Gutsmann, T.; Brandenburg, K.; *Chem. Phys. Lipids* **2009**, *158*, 118.
14. Sani, F. A.; Heidelberg, T.; Hashim, R.; Farhanullah; *Colloids Surf., B* **2012**, *97*, 196.
15. Morita, T.; Fukuoka, T.; Imura, T.; Kitamoto, D.; *Appl. Microbiol. Biotechnol.* **2013**, *97*, 4691.
16. Morita, T.; Fukuoka, T.; Imura, T.; Kitamoto, D.; *J. Oleo Sci.* **2015**, *64*, 133.
17. Lopez, O.; Cocera, M.; Parra, J. L.; de la Maza, A.; *Colloids Surf., A* **2001**, *193*, 221.
18. Lopez, O.; Cocera, M.; Coderch, L.; Parra, J. L.; de la Maza, A.; *Colloid Polym. Sci.* **2002**, *280*, 352.
19. Toro, C.; Sanchez, S. A.; Zanocco, A.; Lemp, E.; Gratton, E.; Gunther, G.; *Chem. Phys. Lipids* **2009**, *157*, 104.
20. Bouwman, L. H.; Roep, B. O.; Roos, A.; *Hum. Immunol.* **2006**, *67*, 247.
21. Blumenstock, E.; Jann, K.; *Infect. Immun.* **1982**, *35*, 264.
22. Matsumura, S.; Imai, K.; Yoshikawa, S.; Kawada, K.; Uchibori, T.; *J. Am. Oil Chem. Soc.* **1990**, *67*, 996.
23. Planas, O.; Bresolí-Obach, R.; Nos, J.; Gallavardin, T.; Ruiz-González, R.; Agut, M.; Nonell, S.; *Molecules* **2015**, *20*, 6284.
24. Yoshimura, T.; Umezawa, S.; Fujino, A.; Torigoe, K.; Sakai, K.; Sakai, H.; Abe, M.; Esumi, K.; *J. Oleo Sci.* **2013**, *62*, 353.
25. Kim, B. S.; Hong, D. J.; Bae, J.; Lee, M.; *J. Am. Chem. Soc.* **2005**, *127*, 16333.
26. Hierrezuelo, J. M.; Molina-Bolivar, J. A.; Carnero-Ruiz, C.; *J. Phys. Chem. B* **2009**, *113*, 7178.
27. Donnelly, M. J.; Bu'Lock, J. D.; *J. Am. Oil Chem. Soc.* **1988**, *65*, 284.
28. Becerra, N.; Toro, C.; Zanocco, A. L.; Lemp, E.; Günther, G.; *Colloids Surf., A* **2008**, *327*, 134.
29. Hill, K.; Rhode, O.; *Fett/Lipid* **1999**, *101*, 25.
30. Gunjikar, J. P.; Ware, A. M.; Momin, S. A.; *J. Dispersion Sci. Technol.* **2006**, *27*, 265.
31. Iwamura, M.; Ishikawa, T.; Koyama, Y.; Sakuma, K.; Iwamura, H.; *Tetrahedron Lett.* **1987**, *28*, 679.

32. Bombelli, C.; Bordi, F.; Borocci, S.; Diociaiuti, M.; Lettieri, R.; Limongelli, F.; Mancini, G.; Sennato, S.; *Soft Matter* **2011**, *7*, 8525.
33. Somerharju, P.; *Chem. Phys. Lipids* **2002**, *116*, 57.
34. Martins, J.; Melo, E.; *Biophys. J.* **2001**, *80*, 832.
35. Chen, S.; Duhamel, J.; Bahun, G. J.; Adronov, A.; *J. Phys. Chem. B* **2011**, *115*, 9921.
36. Nagarajan, S.; Das, T. M.; *New J. Chem.* **2009**, *33*, 2391.
37. Encinas, M. V.; Lemp, E.; Lissi, E. A.; *J. Photochem. Photobiol., B* **1989**, *3*, 113.
38. Schmidt, R.; Tanielian, C.; Dunsbach, R.; Wolff, C.; *J. Photochem. Photobiol., A* **1994**, *79*, 11.
39. De la Fuente, J. R.; Cañete, Á.; Jullian, C.; Saitz, C.; Aliaga, C.; *Photochem. Photobiol.* **2013**, *89*, 1335.
40. National Instruments Corporation; *LabVIEW 8.0*; National Instruments Corporation, Austin, 2005.
41. WaveMetrics; IGOR Pro 6.3; WaveMetrics, Lake Oswego, 2006.
42. Niko, Y.; Kawauchi, S.; Otsu, S.; Tokumaru, K.; Konishi, G.; *J. Org. Chem.* **2013**, *78*, 3196.
43. Lin, I. J.; *J. Phys. Chem.* **1972**, *76*, 2019.
44. Wilkinson, F.; Helman, W. P.; Ross, A. B.; *J. Phys. Chem. Ref. Data* **1993**, *22*, 113.
45. Jimenez-Banzo, A.; Ragas, X.; Kapusta, P.; Nonell, S.; *Photochem. Photobiol. Sci.* **2008**, *7*, 1003.
46. Nonell, S.; Braslavsky, S. E.; *Methods Enzymol.* **2000**, *319*, 37.
47. Chacon, J. N.; Mclearie, J.; Sinclair, R. S.; *Photochem. Photobiol.* **1988**, *47*, 647.
48. Birks, J. B.; Dyson, D. J.; Munro, I. H.; *Proc. R. Soc. London, Ser. A* **1963**, *275*, 575.
49. Leonenko, Z. V.; Finot, E.; Ma, H.; Dahms, T. E. S.; Cramb, D. T.; *Biophys. J.* **2004**, *86*, 3783.
50. Feitosa, E.; Barreleiro, P. C. A.; Olofsson, G.; *Chem. Phys. Lipids* **2000**, *105*, 201.
51. Mori, Y.; Shinoda, H.; Nakano, T.; Kitagawa, T.; *J. Phys. Chem. A* **2002**, *106*, 11750.
52. Getoff, N.; Solar, S.; Richter, U. B.; Haenel, M. W.; *Radiat. Phys. Chem.* **2003**, *66*, 207.
53. Ikeda, S.; Murata, S.; Ishii, K.; Hamaguchi, H.; *Bull. Chem. Soc. Jpn.* **2000**, *73*, 2783.

Submitted: August 3, 2015
Published online: November 10, 2015